Supplementary Information for

In-Petri-dish Acoustic Vortex Tweezers

Teng Li, Yingshan Du, Bowen Cai, Micheal R. Brooks, Chongpeng Qiu, Zhide Wang, Jiali Li, Luyu Bo, Y. Albert Pan, and Zhenhua Tian

Section S1. Design of holographic lenses for generating focused vortex beams

A holographic lens can be considered as a combination of $M \times N$ subwavelength elements distributed on a two-dimensional (2D) grid. The exit of the $(m, n)^{th}$ element is located at $\mathbf{x}_{m,n} = (x_{m,n}, y_{m,n}, 0)$, where m and n are the element indices in the x and y directions, respectively, as illustrated in Fig. S1(a). The element widths Δx and Δy in the x- and y- directions are d. The center of the 2D element array is at the coordinate origin, *i.e.*, $\sum_{m=1}^{M}\sum_{n=1}^{N}\mathbf{x}_{m,n} = \mathbf{0}$. To transform incident plane-wavefront acoustic waves into a focused vortex beam, the thickness profile of a holographic lens should be encoded with the desired phase map, which fuses two components including one phase map for focusing acoustic waves and the other phase map for introducing a vortex with a topological charge number of Q.

To generate a focused acoustic beam with a focal point at $\mathbf{x}_F$, the acoustic waves transmitting through individual elements should arrive at $\mathbf{x}_F$ simultaneously. This can be achieved by setting the phase shift for the $(m, n)^{th}$ element to

$$\Delta\phi_{m,n}^{F} = k_f |\mathbf{x}_F - \mathbf{x}_{m,n}| \tag{S1}$$

On the other hand, to generate an acoustic vortex with a helical wavefront, the holographic lens should be encoded with an angle-dependent phase shift $\delta\varphi_{m,n} = -Q\theta_{m,n}$, where the integer Q is the topological

charge number and $\theta_{m,n}$ is the angle of the $(m, n)^{th}$ element. By fusing the aforementioned two phase components, the total phase shift for generating a focused acoustic vortex beam can be expressed as

$$\Delta\phi_{m,n}^{V} = k_f |\mathbf{x}_F - \mathbf{x}_{m,n}| - Q\theta_{m,n} \tag{S2}$$

where k_f is the wavenumber of acoustic waves in the surrounding medium. Examples of the obtained phase profiles of holographic acoustic lenses for generating focused vortex beams with different topological charge numbers are given in Fig. 2. The phase shifts $\Delta\phi_{m,n}^{V}$ determined by Eq. (S2) may not be in the 0 to 2π range. In order to design an acoustic lens with small thickness changes, the phase shift is compressed to the 0 to 2π range by using the relation $e^{i\Delta\phi} = e^{i(\Delta\phi+2q\pi)}$ where q is an integer.

With the desired phase shift $\Delta\phi_{m,n}^{V}$, we can design a thin holographic acoustic lens for the generation of a focused acoustic vortex beam, by encoding the desired phase shift profile into the holographic lens' thickness profile using the following relation,

$$h_{m,n} = \frac{\Delta\phi_{m,n}^{V}}{k_f - k_{lens}} + h_b \tag{S3}$$

where k_{lens} is the wavenumber of pressure acoustic waves in the lens material, h_b is the lens base's thickness, and $h_{m,n}$ is the thickness of the lens's $(m, n)^{th}$ element. Fig. 2(d) shows thickness profiles of holographic lenses for generating focused vortex beams with topological charge numbers ranging from 1 to 5. With the obtained thickness profile, an acoustic lens can be fabricated by using a high-resolution stereolithography 3D printer (Form 3, Formlabs) with a photocurable resin (RS-F2-GPCL-04, Formlabs). Fig. 3(b) shows 3D printed holographic lenses for generating focused vortex beams with topological charge numbers of 1, 3, and 5.

Section S2. Analytical simulations of focused acoustic vortex beams

To predict the acoustic pressure and intensity fields generated by our holographic acoustic vortex device, we used the following analytical approach. The derivation starts from the analytical model for the acoustic wave transmitted through a subwavelength element of the lens. The transmitted wave is approximated by a spherical wave generated from a point source at the exit of the element. For the $(m, n)^{th}$ element of the holographic acoustic lens, the pressure field of the transmitted acoustic wave with respect to position $\mathbf{x}$ and time t can be expressed as[1,2],

$$p_{m,n}(t,\mathbf{x}) = \frac{Aa_{m,n}e^{i\omega t}}{|\mathbf{x}-\mathbf{x}_{m,n}|} e^{i[-k_f|\mathbf{x}-\mathbf{x}_{m,n}|+\Delta\phi_{m,n}]} \tag{S4}$$

where $a_{m,n}$ is the transmission coefficient introduced by the $(m, n)^{th}$ element. k_f is the wavenumber of pressure waves in the fluid. A and ω are the amplitude and frequency of incident acoustic waves. For positions with $|\mathbf{x}_{m,n}|$ larger than the circular piezoelectric transducer's radius R, the amplitude A should be set to zero in the simulation. $\Delta\phi_{m,n}$ is the phase shift for an incident plane-wavefront acoustic wave that transmits through the holographic lens and then arrives at the lens' exit plane, as illustrated in Fig. S1(b). It can be obtained using the relation $\Delta\phi_{m,n} = -k_{lens}h_{m,n} - k_f(h_{\max} - h_{m,n})$.

By considering the contributions of all the elements of the holographic acoustic lens, we can obtain the total acoustic pressure field expressed as $p(t,\mathbf{x}) = \sum_{m=1}^{M}\sum_{n=1}^{N} p_{m,n}(t,\mathbf{x})$. Then the intensity field can be evaluated by averaging $p(t,\mathbf{x})^2$ in one cycle, expressed as $I(\mathbf{x}) = \left\langle p(t,\mathbf{x})^2 \right\rangle$. The acoustic radiation force $\mathbf{F}$ applied to a small object can be derived using the negative gradient of the Gor'kov potential field U[3,4]. As the Gor'kov potential-based acoustic radiation force calculation method is subjected to the Rayleigh limit, the acoustic radiation force applied on a spherical object over the Rayleigh limit can be calculated using a method established by Sapozhnikov and Bailey[5].

Figures

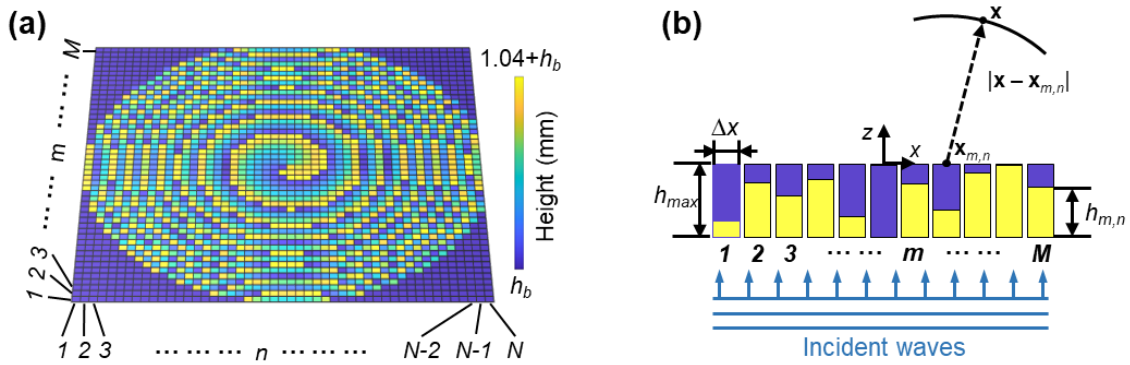

Fig. S1. Schematics for illustrating the lens design and the analytical model. (**a**) Schematic for illustrating the lens design. The holographic lens can be considered as an array of $M \times N$ subwavelength elements (or pixels). (**b**) 2D schematic in the x-z plane for developing the analytical model. As incident acoustic waves transmit through each element, the phase changes in both the lens (yellow) and fluid (purple) sections should be considered. The total phase change for the $(m, n)^{th}$ element with an exit located at $\mathbf{x}_{m,n}$ should be $\Delta\phi_{m,n} = -k_{lens} h_{m,n} - k_f (h_{\max} - h_{m,n})$, where k_{lens} and k_f are the wavenumbers in the lens and fluid regions. $h_{\max}$ and $h_{m,n}$ are the maximum lens height and the $(m, n)^{th}$ element's height.

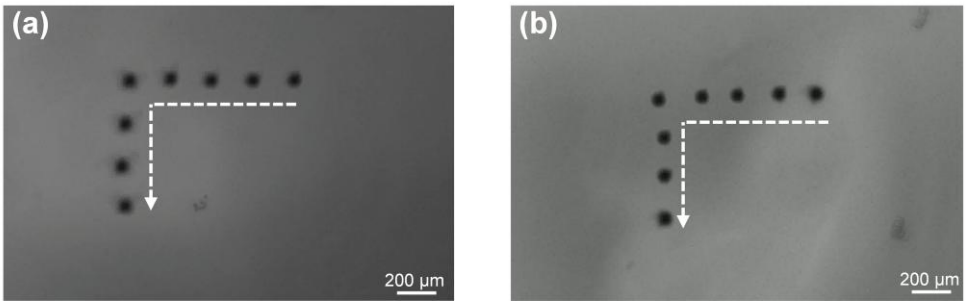

Fig. S2. Experimental results (stacked microscopic images) showing that 75 μm microparticles were trapped and translated by an acoustic vortex beam after transmitting through two plates: (a) 0.9 mm glass and **(b)** 2.6 mm acrylic plates.

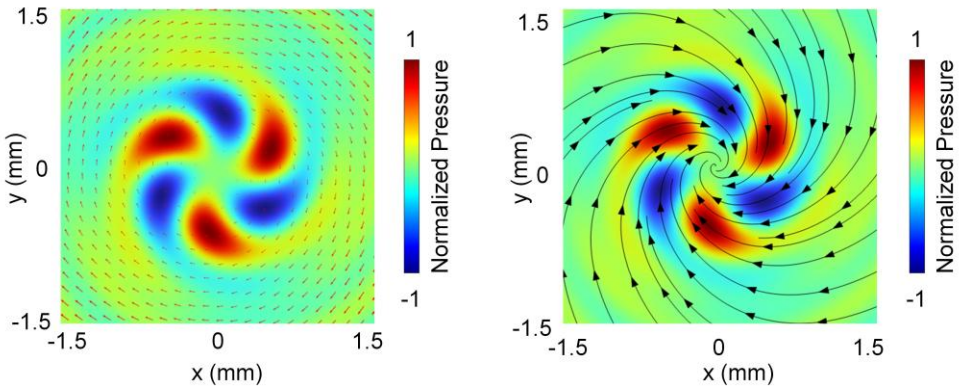

Fig. S3. Simulated acoustic streaming fields induced by a vortex beam with a topological charge number of 3. The arrows in the left figure represent streaming velocity vectors. The lines in the right figure represent streamlines. The background color image reveals the acoustic pressure field.

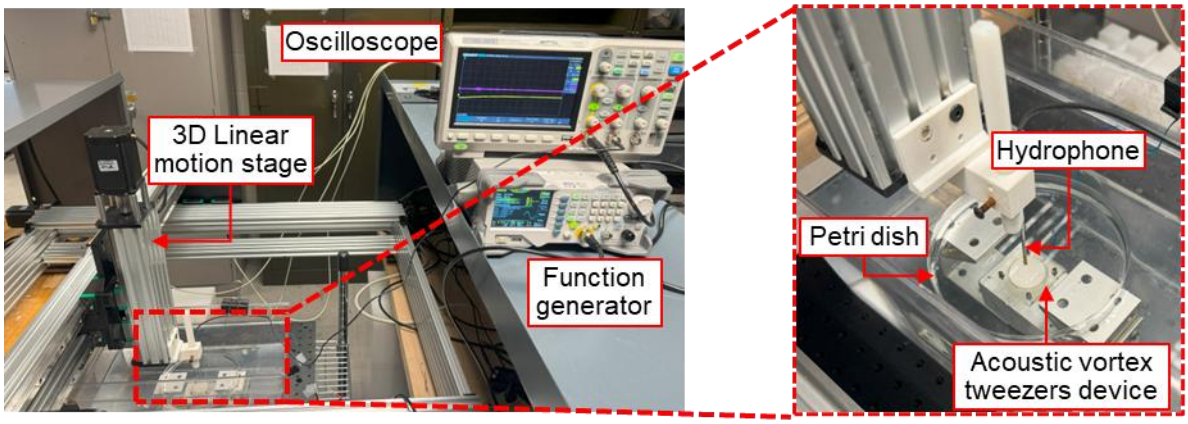

Fig. S4. Photos of a test setup for acoustic field characterization. The test setup uses a function generator (DG 1022Z, RIGOL) to send an excitation signal to the acoustic tweezers device underneath a Petri dish, an oscilloscope (SDS 1202-E, SIGLENT) to acquire acoustic signals from a needle-type hydrophone (HNR-0500, ONDA Co.), as well as a 3D linear motion stage to change the hydrophone locations for point-by-point data acquisition.

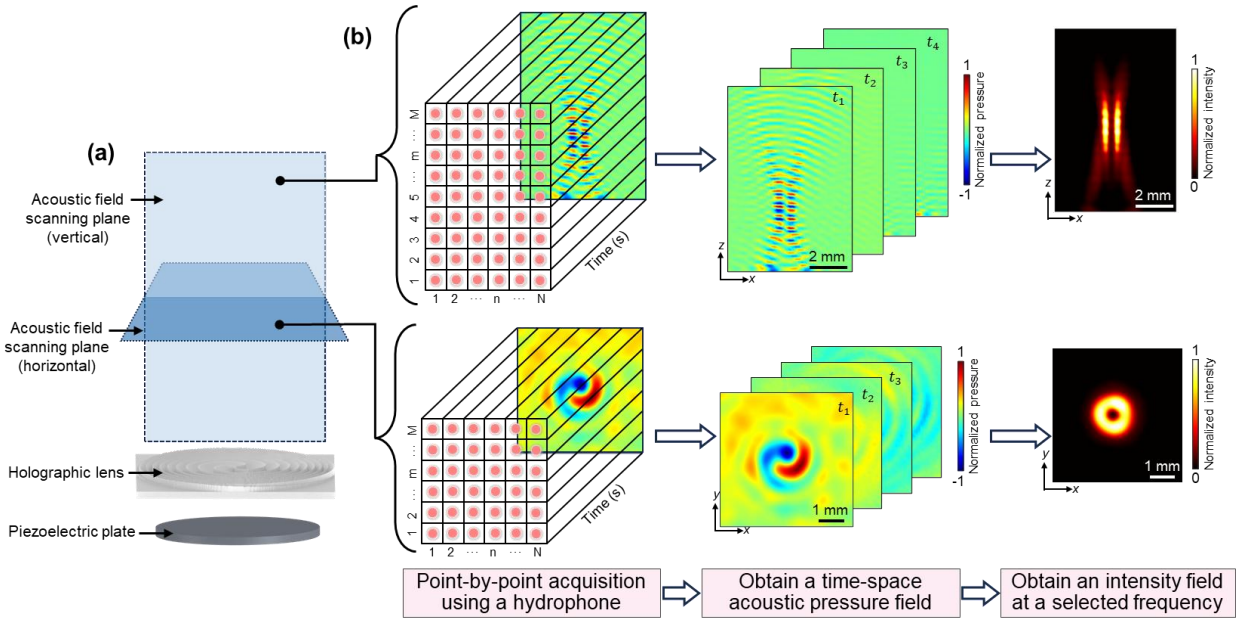

Fig. S5. Procedures for characterizing acoustic fields. (**a**) A schematic showing the vertical and horizontal planes for acoustic field acquisition. (**b**) Procedures for obtaining pressure and intensity fields. Through point-by-point scanning, waveforms at numerous scanning points can be acquired. The combination of these waveforms gives a time-space wavefield $S_{ts}(t, \mathbf{x})$. By applying the Fourier transform to the time-space wavefield, we can further obtain a frequency-space wavefield $S_{fs}(f, \mathbf{x})$. Then we can obtain an intensity field $|S_{fs}(f_i, \mathrm{x})|^2$ at a selected frequency of f_i.

Legends for Movies S1 to S10

Movie S1. Particle aggregation enabled by shrinking an acoustic potential well. By shrinking the potential well diameter, microparticles in a Petri dish were gradually concentrated.

Movie S2. Trapping and translating a microparticle. A 75 μm polystyrene sphere in a Petri dish was trapped by a focused vortex beam with a topological charge number of Q=1 and then translated along complex paths to write 'VORTEX'.

Movie S3. Trapping flowing microparticles to gradually create a particle cluster. Flowing microparticles were gradually trapped by an acoustic potential well induced by a focused vortex beam with a topological charge number of Q=3 to create a particle cluster, whose diameter gradually increased to ~0.9 mm.

Movie S4. Translating a particle cluster. A cluster of microparticles in a Petri dish was trapped and translated tracing complex paths to write 'VHAND'.

Movie S5. Concentrating cells. Cells were trapped by acoustic vortex tweezers to gradually form a cell cluster in a Petri dish.

Movie S6. Translating a cluster of cells. A cluster of cells was trapped and translated along complex paths to write 'V' in a Petri dish.

Movie S7. Trapping and translating a zebrafish larva in a horizontal posture. A zebrafish larva was horizontally trapped and then transported along programmed trajectories to write the letters 'ZEBRA'.

Movie S8. Trapping and translating a zebrafish larva in a vertical posture. A zebrafish larva was vertically trapped and then transported along programmed trajectories to write the letters 'ZEBRA'.

Movie S9. Rotating acoustically trapped zebrafish larvae. Acoustically trapped zebrafish larvae in horizontal and vertical postures were rotated in the clockwise direction.

Movie S10. Rotating a zebrafish larva for taking images from different angles. A zebrafish larva is rotated by an asymmetric acoustic field.

References

1. B. A. Auld, *Acoustic fields and waves in solids* (John Wiley & Sons Inc., 1973).
2. J. L. Rose, *Ultrasonic waves in solid media* (Cambridge Univ. Press, 1999).
3. L. P. Gor'kov, Soviet Physics Doklady **6**, 733 (1962).
4. H. Bruus, *Lab a Chip*, 2012, **12**, 1014–1021.
5. O. A. Sapozhnikov and M. R. Bailey, *J. Acoust. Soc. Am.*, 2013, **133**, 661–676.